SPACE TELESCOPE SCIENCE INSTITUTE
Operated for NASA by AURA

Instrument Science Report WFC3 2012-14

Breathing, Position Drift, and PSF Variations on the UVIS Detector

L. Dressel
July 13, 2012

ABSTRACT

This study has been undertaken to inform observers of factors that limit the accuracy of execution of small dither patterns and the stability of the UVIS point spread function (psf) over the time span of HST orbits. The position drift of stars in a series of consecutive exposures and the continual change in focus over the course of an orbit have been quantified for the WFC3/UVIS detector using data that finely samples the orbit. Position variations, typically covering a range of 0.1 to 0.2 UVIS pixels per coordinate within an orbit, occurred in complex repeatable patterns in consecutive orbits. These variations limit the accuracy with which small psf-sampling dithers can be executed even within one orbit, where reacquisition errors are not a factor. Focus variations, usually covering a range corresponding to a change in spacing of several microns between the HST secondary and primary mirrors, occurred in periodic patterns in consecutive orbits. The width of the psf is correlated with the focus, and generally changes measurably during an orbit. The dependence of the encircled energy of the psf on focus is quantified for several aperture sizes for filter F420M over the range of focus (9 microns) encountered in the data analyzed here. The focus model maintained by STScI is used to illustrate how focus changes on the timescale of minutes to months to give observers an idea of what they may expect to encounter in their observations.

1. Introduction

Small scale changes in focus occur continuously throughout the course of an HST orbit, a phenomenon referred to as breathing. Stellar images drift slightly on the detector

and change in size in a series of consecutive exposures. The magnitude of these effects depends on the changing thermal environment of the telescope, which is monitored by a variety of sensors. A model of the dependence of focus on the thermal history of the telescope has been developed by analyzing point spread functions (psfs) in imaging exposures and relating them to thermal data gathered over many years of HST operations. Some of the visits in the Optical Monitor program 11877 were designed to check focus changes on the timescale of minutes over periods of two orbits. I have analyzed data from these visits to quantify the position drift and the changes in the encircled energy of stellar images and to relate them to the measured values and model predictions of focus.

2. Data

The data analyzed here were acquired in visits 43 to 50 (datasets ibcy43* to ibcy50*) in CAL/OTA program 11877. A trio of stars in the open cluster NGC 188 was imaged through the F410M filter on a 512x512 pixel subarray (20x20 arcsec) near the center of the WFC3/UVIS detector. Pairs of consecutive visits were made every 12 to 16 days near the end of 2010 (Nov 8, Nov 22, Dec 8, Dec 20). Each visit was executed within a single orbit and consisted of a continuous sequence of 39 exposures of 15 sec each. Calibrated images of the initial exposures in visits 43, 45, 47, and 49 are shown in Figures 1 to 4. The central star in the trio was the designated target. The aperture can be seen to rotate about that star as the roll angle changes from one pair of visits to the next. The position angle of the aperture is the same to within 0.07 degrees for the two visits in a pair.

The three stars were well exposed and unsaturated, with a maximum peak pixel flux of 4000, 13000, and 28000 electrons. Each exposure was cleaned of cosmic rays by comparing it to a cosmic-ray cleaned image made from all 39 exposures in the same visit. The central 11x11 pixels of each stellar image were excluded from cosmic-ray cleaning since small offsets of the psf and changes in focus result in false detections of cosmic rays when high signal-to-noise psfs are compared. The probability of a cosmic ray hit on this small block of pixels in a 15 sec exposure is low, and only one stellar core was clearly impacted.

The 15 sec exposures are just long enough to keep the initial vibration driven by the shutter mechanism from significantly affecting the measurements. The shutter blade rotates 180 degrees for each new exposure, and the vibration lasts longer for one positioning of the blade than for the other (Hartig 2008). For exposures shorter than about 10 sec, greater elongation of the psf can be seen in alternating exposures (Sabbi 2009).

The jitter files were checked for anomalously large values of the rms in V2 and V3. Values several times larger than the typical value of 4 or 5 milliarcsec were found in only 5 of the 312 exposures. As pointed out by Gilliland (2005a), the psfs themselves are a more reliable indicator of anomalous jitter than the jitter files are.

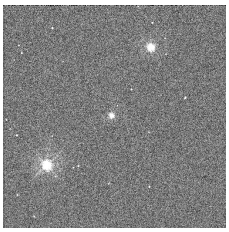

Figure 1. The first flt image (20 x 20 arcsec) of NGC 188 in visit 43, representative of the 78 exposures in visits 43 and 44 with aperture position angle of 12 degrees.

Figure 2. The first flt image (20 x 20 arcsec) of NGC 188 in visit 45, representative of the 78 exposures in visits 45 and 46 with aperture position angle of -2 degrees.

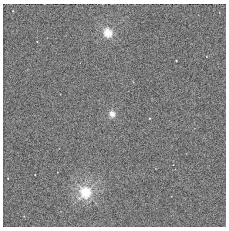

Figure 3. The first flt image (20 x 20 arcsec) of NGC 188 in visit 47, representative of the 78 exposures in visits 47 and 48 with aperture position angle of -20 degrees.

Figure 4. The first flt image (20 x 20 arcsec) of NGC 188 in visit 49, representative of the 78 exposures in visits 49 and 50 with aperture position angle of -34 degrees.

3. Analysis

3.1 Focus

The variation in focus over a visit is generally referred to as breathing, since it tends to be a periodic fluctuation over consecutive orbits. It is driven by variations in the thermal environment of the telescope, which affect the spacing between the HST primary and secondary mirrors. One micron displacement of the secondary mirror from best focus displaces the HST focal plane by an amount that produces an rms wavefront error of 6.1 nm (Di Nino et al. 2008). The technique of phase retrieval is applied to stellar images to measure the wavefront error (Krist and Burrows 1995), which is then generally reported as focus or "despace" in units of microns of displacement of the secondary mirror.

An early paper on the development of HST focus models (SESD-97-01 by Hershey 1997) beautifully illustrates the dependence of breathing structure on the magnitudes and relative phases of the orbital day cycle and the earth occultation cycle. The telescope is heated by the sun during orbital day by an amount that depends on its orientation with respect to the sun (from broadside to end-on) and on its roll angle. (Off-nominal roll places the telescope in an orientation that reduces the shadowing of the front end by the aperture door.) During occultation of the target by the earth, the front end of the telescope receives IR radiation from the earth, with the heating and length of exposure depending on the orientation of the telescope. These two heating cycles drive temperature fluctuations on the timescale of orbits. Depending on the relative orientations of the sun, earth, and target, the cycles can be more nearly in phase, acting together to produce large fluctuations in temperature and focus, or out of phase, canceling to some extent, resulting in smaller fluctuations. A large change in pointing, with a large difference in the heating amplitudes and in the relative phases of these cycles, can cause a temperature drift on the timescale of many orbits.

The focus of each exposure in the calibration program 11877 has been measured by the telescopes group at STScI as part of the on-going focus monitor program (Niemi and Lallo 2010). The measurements are being used to check and refine a model of the dependence of focus on the short-term and long-term thermal and mechanical history of the telescope (Di Nino et al. 2008, Cox and Niemi 2011). The measurements and model predictions can be retrieved using the web tool linked to http://www.stsci.edu/hst/observatory/focus/FocusModel. (For most HST observations, only the model prediction is available.) The posted measurements are generally a combination of the measurements of all the bright stars in an image. For the three stars in the visits examined here, the phase retrieval results are generally the most stable for the brightest star. The focus measured for that star and the model prediction are shown for each visit in the lowest panel of Figures 5 through 8. The deviations of the model from the measurements are usually less than 2 microns, and always less than 4 microns, consistent with the performance analysis of the model by Cox and Niemi (2011). Figures 9 and 10 illustrate the focus model over the course of an entire day for the visits with the greatest variation (visits 45 and 46) and the least variation (visits 47 and 48) in focus.

The focus during the "external" (observing) portions of these visits is over-plotted with a solid line to show the cadence of the breathing with internal and external orbits.

3.2 Position Drift

The positions of stellar images on a detector drift slightly in response to thermal variations in the instrument. These variations are driven by the attitude-based thermal environment of the telescope, but can also be affected by the operation of the instrument and the telescope. STIS, for example, is affected by the cycling on and off of the MAMA electronics and the operation of heaters (Gull et al. 1997). For WFC3, it was anticipated that position drift would largely be driven by the HST thermal environment. This relationship was investigated during the Servicing Mission Orbital Verification (Brown 2009). Two globular clusters were observed in a continuous set of visits over a period of 21 hours each. One cluster was observed at a "hot" thermal attitude ($\sim$99 degrees from target to sun) and the other at a "cold" thermal attitude ($\sim$166 degrees from target to sun). When two-orbit visits within this sequence were considered independently, maximum excursions of 0.35 pixels (14 milliarcsec) and 0.26 pixels (11 milliarcsec) were found near the end of the hot and cold visits, respectively. The analysis of the visits as continuous sequences for each target revealed a long term position drift, totaling 1.3 pixels (50 milliarcsec) over the first 21 hours at the hot attitude, and 0.6 pixels (25 milliarcsec) over the next 21 hours at the cold attitude.

The data from program 11877 give us the opportunity to compare position drift and measured focus variation using data that finely samples the orbit. The visits were designed to optimize phase retrieval analysis for the focus measurements, discussed above, taking exposures long enough to be insensitive to the initial shutter-driven vibration and avoiding the less optically stable portion of the detector near the A amplifier. The positions of the stars in x and in y were measured by summing the data over the 7 brightest rows and the 7 brightest columns, respectively, and fitting a gaussian to the profiles. The x and y positions of the two brightest stars relative to their medians for the visit are plotted for each visit in the upper two panels of Figures 5 through 8. The consistency of the relative positions for the two stars shows that the measuring errors are small compared to the drift. The positions of the third star were similar to these, but showed noticeably more dispersion because of the lower signal to noise. The distance from the median position for each star is plotted for each visit in the third panel of each column in Figures 5 through 8. These are to be compared to the measured and modeled focus displayed in the bottom panel of the figures.

The breathing and drift are seen to be highly repeatable in the consecutive orbits displayed in the left and right columns of Figures 5 through 8. The range of the drift is correlated with the magnitude of the focus change over the orbit. The focus was nearly constant and the stellar positions were most stable in the third pair of visits, 47 and 48. The focus changed the most (6 microns), and the drift was largest ($\sim$0.2 pixels in each coordinate), in the second pair of visits, 45 and 46. In the remaining visits, with an intermediate degree of focus change, the drift was 0.1 to 0.2 pixels per coordinate.

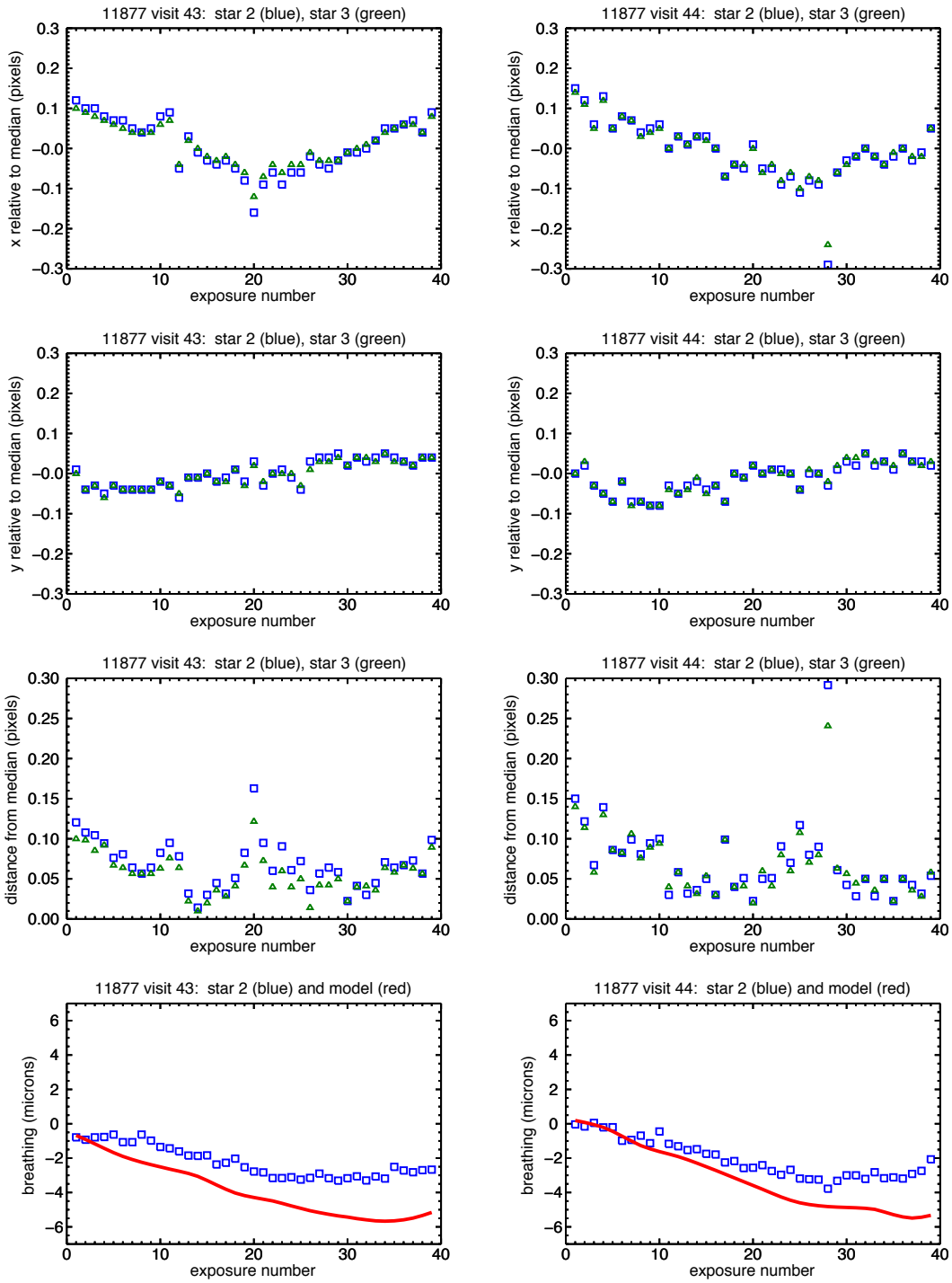

Figure 5. For 11877 visits 43 (left column) and 44 (right column): Drift in x (top panel), drift in y (next panel), and total drift (next panel) relative to the median position in the visit for the brightest two stars; measured focus for the brightest star (squares) and modeled focus (red line) (bottom panel).

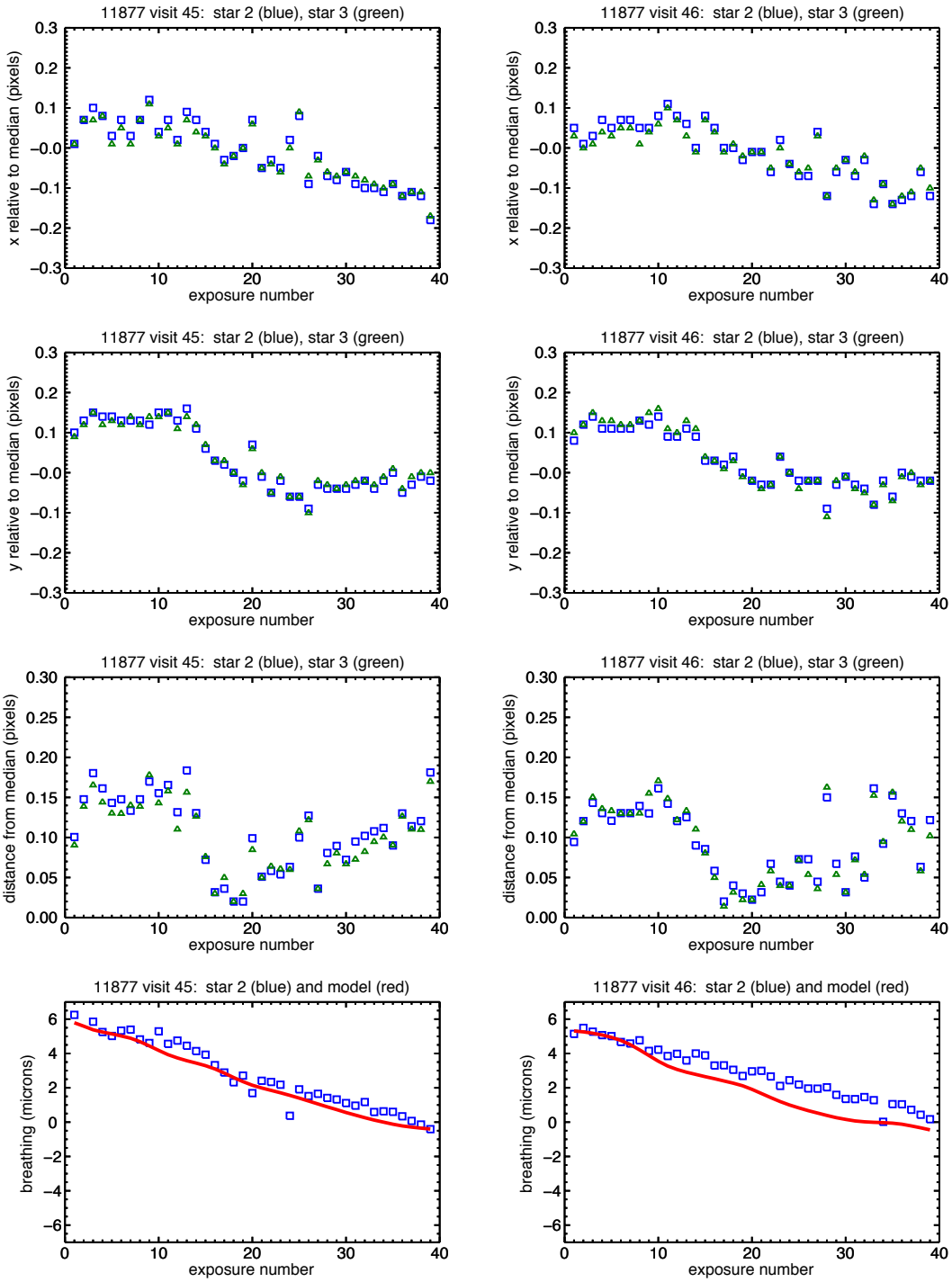

Figure 6. For 11877 visits 45 (left column) and 46 (right column): Drift in x (top panel), drift in y (next panel), and total drift (next panel) relative to the median position in the visit for the brightest two stars; measured focus for the brightest star (squares) and modeled focus (red line) (bottom panel).

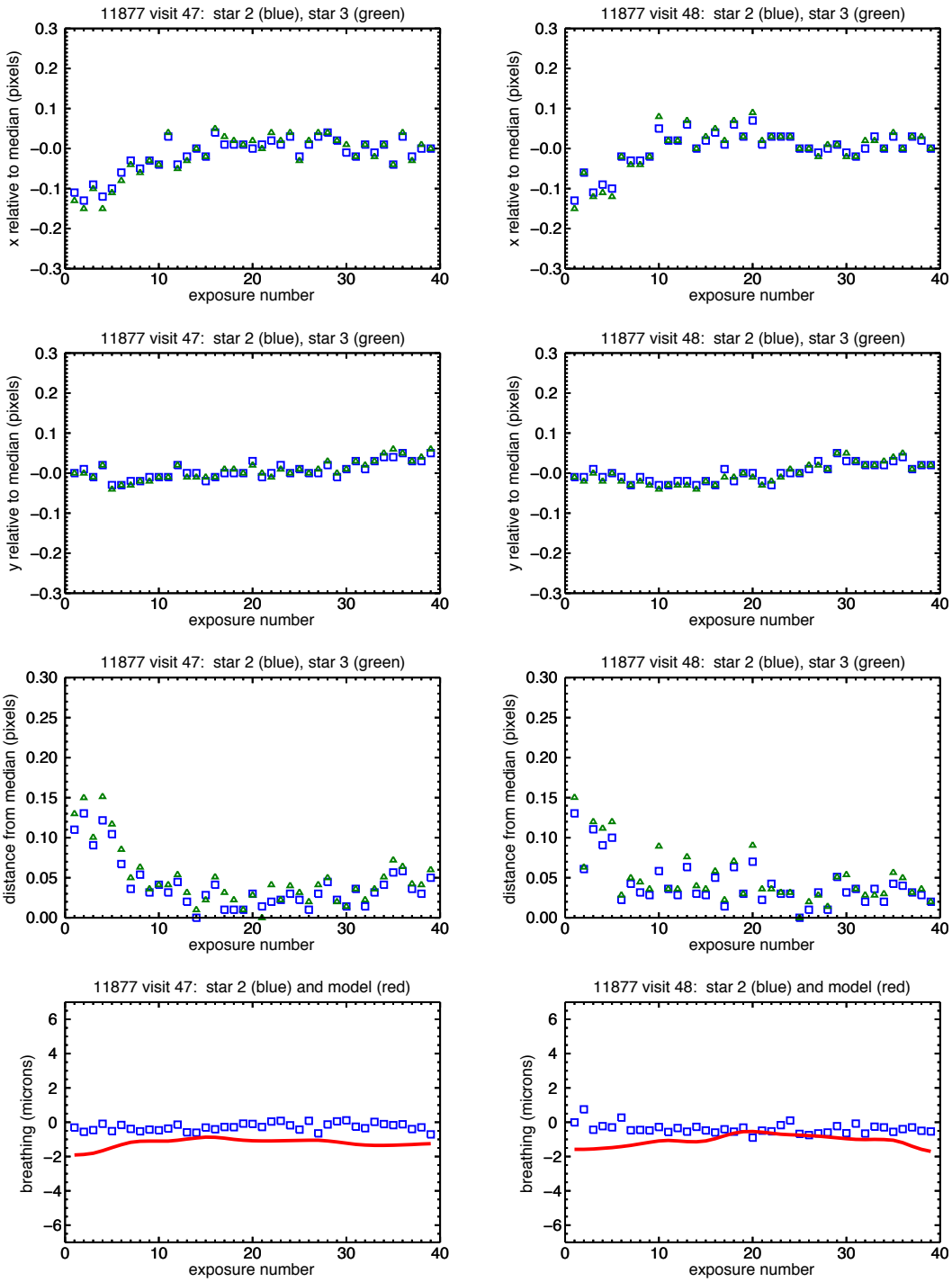

Figure 7. For 11877 visits 47 (left column) and 48 (right column): Drift in x (top panel), drift in y (next panel), and total drift (next panel) relative to the median position in the visit for the brightest two stars; measured focus for the brightest star (squares) and modeled focus (red line) (bottom panel).

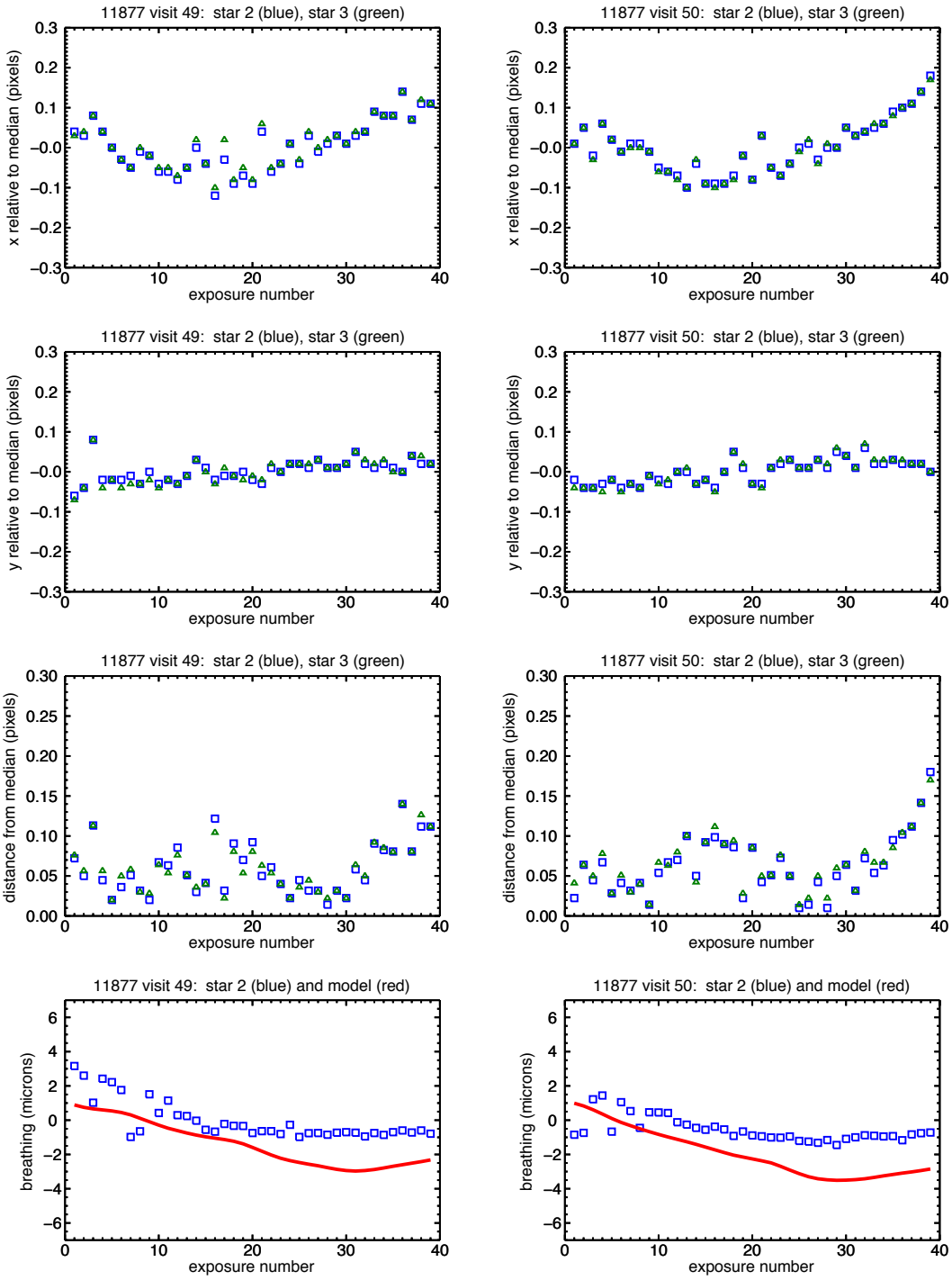

Figure 8. For 11877 visits 49 (left column) and 50 (right column): Drift in x (top panel), drift in y (next panel), and total drift (next panel) relative to the median position in the visit for the brightest two stars; measured focus for the brightest star (squares) and modeled focus (red line) (bottom panel).

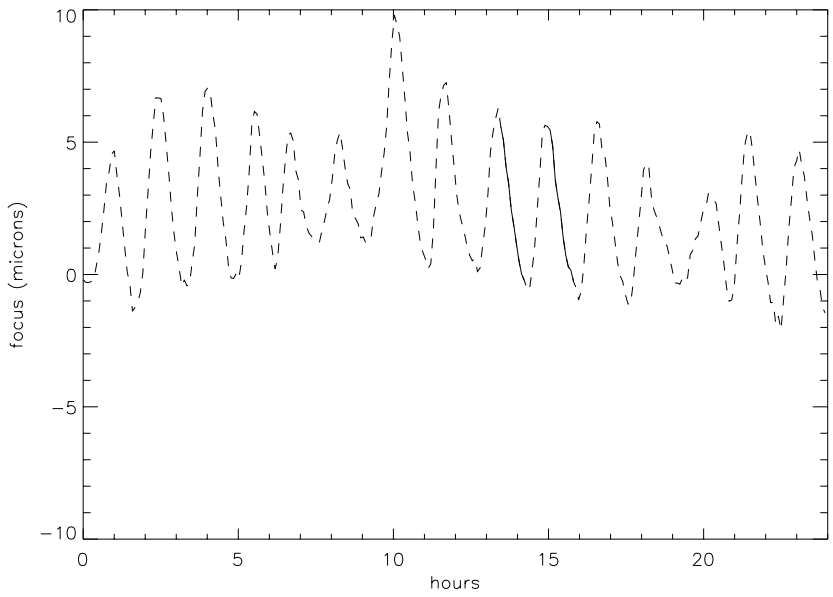

Figure 9. Focus model, determined at 5 minute intervals, for 22 November 2010. The time spans of visits 45 and 46, each one external orbit in length, are indicated by the solid lines.

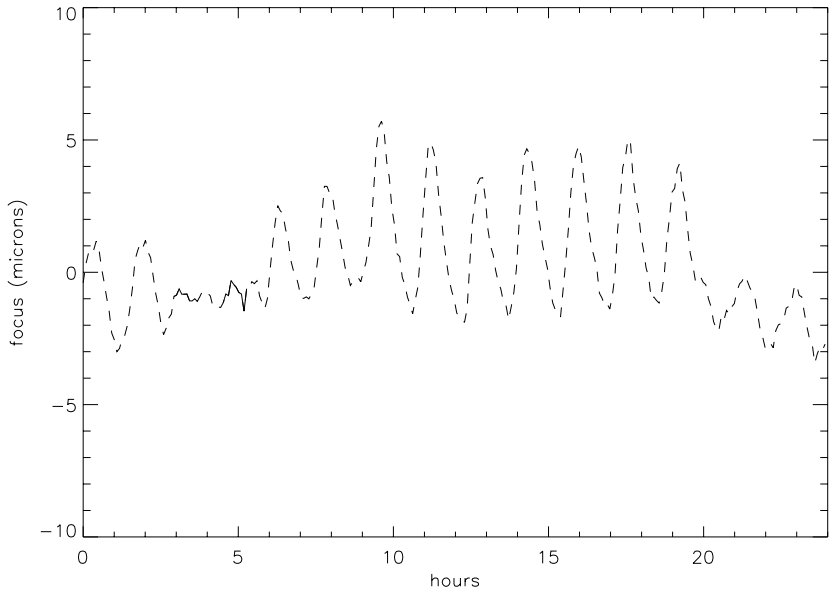

Figure 10. Focus model, determined at 5 minute intervals, for 8 December 2010. The time spans of visits 47 and 48, each one external orbit in length, are indicated by the solid lines.

Similar magnitudes of drift were measured on images from several HST detectors by Gilliland (2005b). His analysis of dithered exposures lead him to conclude that the errors in offsets executed with small POS TARGs are insignificantly small compared to the drift. (Offsets of less than 1 arcsec within a orbit have a typical rms accuracy of 2 to 5 milliarcsec (Fruchter, Sosey et al. 2009).) The typical drift limits the accuracy of psf sampling with small dither patterns. Additionally, non-linear distortion, significant for the WFC3 detectors, causes the step size of dithers in pixels to vary over the detector with greater magnitude as the step size increases (Dressel (2011) Appendix B and C).

The visits examined here were made at hot thermal attitudes ($\sim$113 degrees from target to sun). In these one-orbit visits, the maximum excursion (excluding one clearly aberrant point) was under 0.20 pixels (8 milliarcsec). This is consistent with the SMOV results for two-orbit visits (Brown 2009), given the uncertainty of 5 to 20 milliarcsec in reacquisitions for consecutive orbits in the same visit (Fruchter, Sosey et al. 2009).

3.3 Encircled Energy

The fraction of the flux of a point source contained in an aperture a few pixels in diameter can change substantially over the course of an orbit as the focus changes. Encircled energies within diameters of 0.15, 0.20, and 0.25 arcsec (3.8, 5.0, and 6.3 pixels) were measured using software developed to assess image quality (Hartig 2009). For pixels that lie on the border of the aperture, the flux is divided according to the fraction of the pixel included by the aperture. The encircled energy fractions are plotted in Figure 11 as a function of the measured focus for the brightest star imaged in visits 43 and 44 (focus $\sim$ -3.3 to 0.0 microns) and visits 45 and 46 (focus $\sim$ -0.4 to 6.0 microns). The focus was measured allowing the spherical aberration and the CCD charge diffusion to be fit as free parameters, when they should be constant at a given location on the detector. Over the limited range of excursions from best focus experienced in normal operations, differences in the psf due to differences in the focus, spherical aberration, and charge diffusion components are difficult to distinguish, so unrealistic trade-offs in the fits of these components occur when all are unconstrained. Experimentation with fixing the spherical aberration and charge diffusion to a typical pair of values produced changes of up to 1 micron in the focus fits. This should be kept in mind when interpreting Figure 11.

The encircled energy curves in Figure 11 peak at a focus value $\sim$0 microns, confirming that best focus occurred at focus $\sim$0 microns as determined via phase retrieval analysis. This supports the estimate by Niemi and Lallo (2010), with several caveats, that the typical focus of the WFC3/UVIS detector passed through the optimal value (slowly moving to negative values) between March and October 2010. The modeled focus for the month of November 2010 is plotted in Figure 12, to show the structure of fluctuations encountered in a typical month. Figure 13 shows a normalized histogram of the modeled focus in November and December 2010, the months in which the observations analyzed in this ISR were made. The mean and rms of the modeled focus values in this time range are -0.1 micron and 2.8 microns. A typical orbit spans several microns

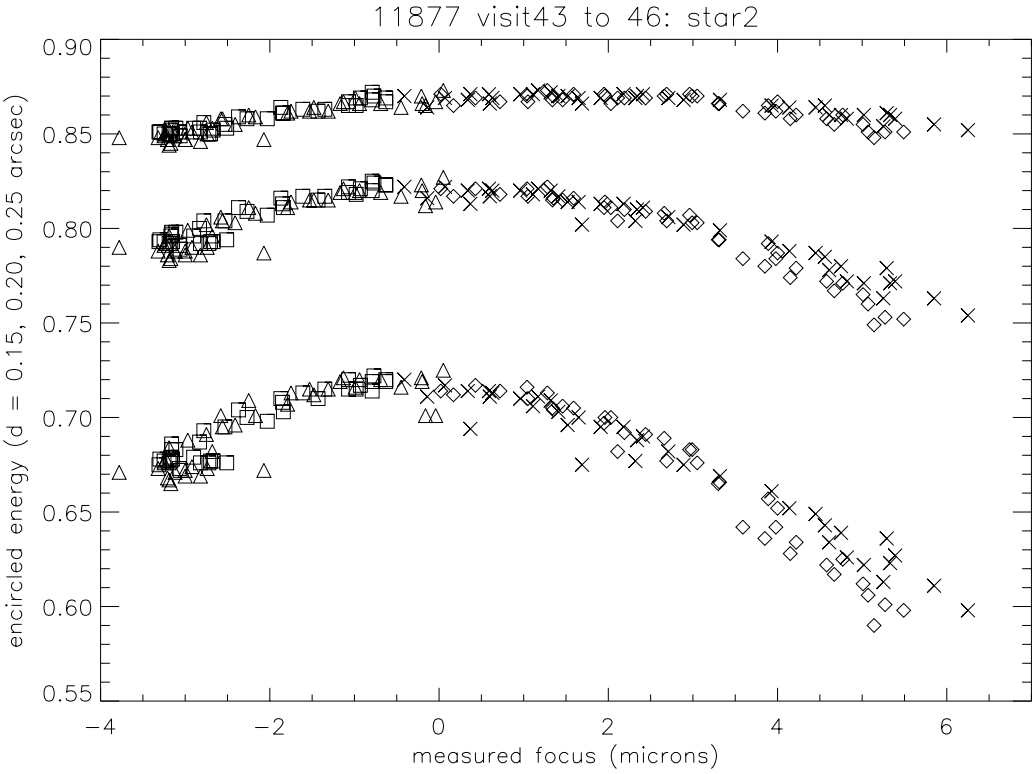

Figure 11. Fraction of energy encircled by 3 apertures (diameters = 0.15, 0.20, 0.25 arcsec) vs focus measured via phase retrieval (microns of despace) for the brightest star in visits 43 (square), 44 (triangle), 45 (x), and 46 (diamond) of program 11877.

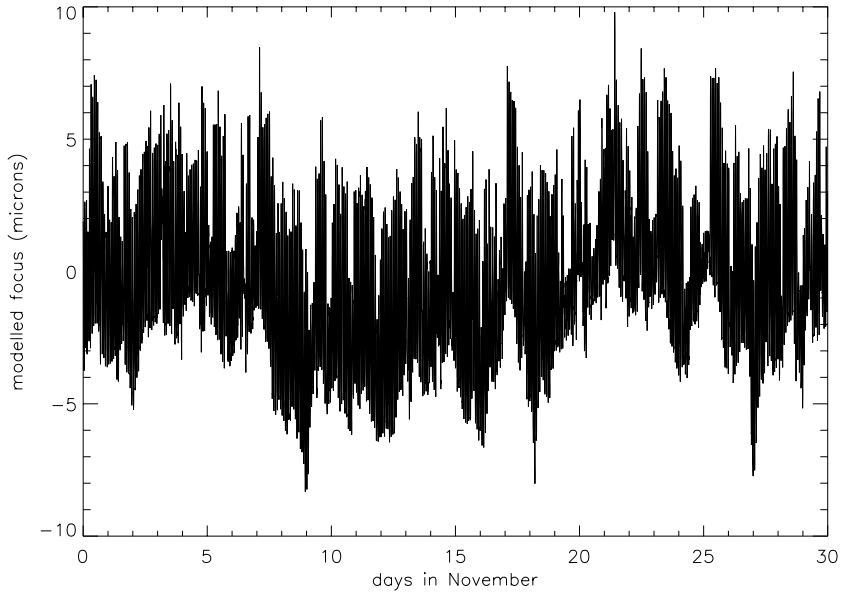

Figure 12. Modeled focus (microns) in November 2010, determined at 5 minute intervals. (See Figures 9 and 10 for structure on the order of orbits and days.)

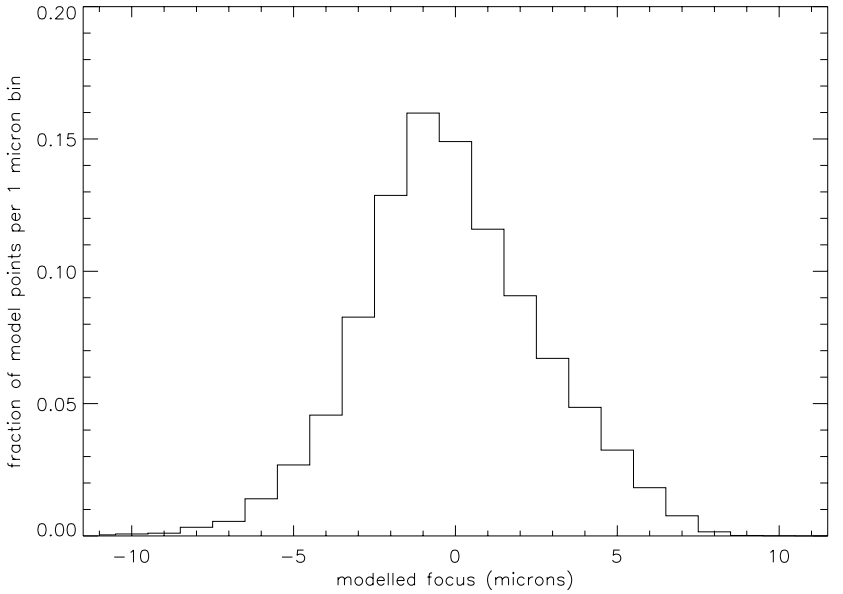

Figure 13. Normalized histogram of modeled focus in November and December 2010, the months in which the observations analyzed in this ISR were made.

in focus and experiences values of focus somewhere between -6 and +6 microns.

4. Conclusions

Drift of the positions of stars in images and change in focus can be highly repeatable in series of exposures taken in consecutive HST orbits. The structure of the drift is complex, and typically covers a range of 0.1 to 0.2 pixels per coordinate on the WFC3/UVIS detector during the course of an orbit. This limits the accuracy with which small psf-sampling dithers can be executed, even within one orbit. Reacquisitions in subsequent orbits of the same visit introduce additional offsets of 0.13 to 0.5 pixels (5 to 20 milliarcsec). When observations of a target continue for many hours, there is a long term position drift whose magnitude depends on the thermal state of the telescope. A previous study found total drifts ranging from 0.6 pixels (25 milliarcsec) to 1.3 pixels (50 milliarcsec) over periods of 21 hours.

Change in focus is generally periodic on the timescale of an orbit. It is caused by a thermally driven change in the spacing between the HST secondary and primary mirrors, which typically varies by several microns in one orbit. The amplitude and mean value of the fluctuation in focus can change from orbit to orbit, especially after a significant change in spacecraft pointing. The psf width and encircled energies are correlated with the focus, and generally change measurably during an orbit. For long exposures, the drift in position also affects the size and shape of the psf. (For exposures shorter than about 15 seconds, initial vibration driven by the UVIS shutter mechanism causes elongation of the psf.) Modeled values of the focus based on HST thermal data (http://www.stsci.edu/hst/observatory/focus/FocusModel) are made available to the community to assist observers in interpreting the optical quality of their images.

Observers need to keep in mind that position drift will limit their ability to uniformly sample the psf in a small number of dithered exposures. Position drift and acquisition errors will limit their ability to accurately plan dithers over many orbits or visits. Position drift and focus change will have to be taken into account when planning programs that depend on accurate psf measurement or subtraction. The tendency of repeatability of drift and focus in consecutive orbits of a visit cannot necessarily be counted on in the execution of phase II proposals, since the “orbits” that are defined in APT can be interrupted or broken up in the scheduling process.

5. Acknowledgments

I thank Sami Niemi and Colin Cox for introducing me to the phase retrieval software used at STScI, and John Biretta for reviewing this document.

References

Brown, T. 2009, "WFC3 SMOV Proposal 11549: Image Stability", STScI ISR WFC3 2009-32

Cox, C., and Niemi, S.-M. 2011, "Evaluation of a temperature-based HST Focus Model", STScI ISR TEL 2011-01

Di Nino, D., Makidon, R.B., Lallo, M., Sahu, K.C., Sirianni, M., and Casertano, S. 2008, "HST Focus Variations with Temperature", STScI ISR ACS 2008-03

Dressel, L. 2011. "Wide Field Camera 3 Instrument Handbook, Version 4.0" (Baltimore: STScI), http://www.stsci.edu/hst/wfc3/documents/handbooks/currentIHB

Fruchter, A., Sosey, M. et al. 2009, "The MultiDrizzle Handbook", version 3.0, (Baltimore, STScI)

Gilliland, R.L. 2005a, "Observer Anomaly(?): Recent Jitter and PSF Variations', STScI ISR TEL 2005-01

Gilliland, R.L. 2005b, "Guiding Errors in 3-Gyro: Experience from WF/PC, WFPC2, STIS, NICMOS and ACS", STScI ISR TEL 2005-02

Gull, T.R., Taylor, M.J., Shaw, R., Robinson, R., and Hill, R.S. 1997, "Thermal Motion of the STIS Optical Bench", in The 1997 HST Calibrtion Workshop Proceedings, http://www.stsci.edu/institute/conference/cal97/proceedings.html

Hartig, G.F. 2008, "WFC UVIS Shutter Vibration-Induced Image Blur", STScI ISR WFC3 2008-44

Hartig, G.F. 2009, "WFC3 SMOV Programs 11436/8: UVIS On-orbit PSF Evaluation", STScI ISR WFC3 2009-38

Hershey, J.L. 1997, "Modeling HST Focal-Length Variations", STScI SESD 97-01, http://www.stsci.edu/institute/org/telescopes/Reports/isrs/sesdrep.pdf

Krist, J. and Burrows, C.J. 1995, "Phase Retrieval Analysis of pre-and post-repair Hubble Space Telescope Images", Appl. Opt. 34, 4951.

Niemi, S.-M., and Lallo, M. 2010, "Phase Retrieval to Monitor HST Focus: II. Results Post-Servicing Mission 4", STScI ISR TEL 2010-03

Sabbi, E. 2009, "WFC3 SMOV Program 11798: UVIS PSF Core Modulation", STScI ISR WFC3 2009-20